Chapter 4
Reduced-Order Modeling

M. Valášek, Z. Šika, T. Vampola and S. Hecker

4.1 Model Order Reduction

M. Valášek, Z. Šika and T. Vampola

4.1.1 General Process of Generation of Parameterized Reduced-Order Models for Control Design

The output of the complex modeling process without reduction is the full model of the ACFA BWB aircraft predesign model in the original unreduced number of coordinates that is known for many discrete values of parameters $\mathbf{p}_\mathrm{d}$. It is supposed that the original models are linear and represented in the state-space form

$$\begin{aligned}\dot{\mathbf{x}}_\mathrm{F} &= \mathbf{A}_\mathrm{F}(\mathbf{p}_\mathrm{d})\mathbf{x}_\mathrm{F} + \mathbf{B}_\mathrm{F}(\mathbf{p}_\mathrm{d})\mathbf{u}\\ \mathbf{y} &= \mathbf{C}_\mathrm{F}(\mathbf{p}_\mathrm{d})\mathbf{x}_\mathrm{F} + \mathbf{D}_\mathrm{F}(\mathbf{p}_\mathrm{d})\mathbf{u}.\end{aligned} \tag{4.1}$$

The differential equations over structural and aerodynamic degrees of freedom (states) are given by the system matrix **A**. The state variables **x** are related to an input vector **u** containing input quantities, for example, control surface actuation moments, by the control matrix **B**. The transformation from states to outputs **y** is achieved by the observation matrix **C**. In case, inputs have a direct effect on the outputs, the feedthrough matrix **D** can be included. The index F indicates the full set of degrees of freedom.

M. Valášek (✉) · Z. Šika · T. Vampola
Czech Technical University in Prague, Prague, Czech Republic
e-mail: michael.valasek@fs.cvut.cz

S. Hecker
Munich University of Applied Sciences, Munich, Germany

M. Kozek and A. Schirrer (eds.), *Modeling and Control for a Blended Wing Body Aircraft*,
Advances in Industrial Control, DOI 10.1007/978-3-319-10792-9_4

Nevertheless, the unreduced version of the parameterized model is totally unusable for the control law synthesis. The suitable reduction can be done generally in two main steps. First, the full structural model is reduced based on the modal coordinates taken into account the relatively wide frequency range. The upper preserved frequencies after the first step of the reduction should be sufficiently high (for example, about 30 Hz). The rejected modes can either be completely neglected or partially taken into account by singular perturbation approximation (SPA), without enlarging the model order. All rigid body (RB) modes of the structure as a whole have to be preserved, since they are base for the flight mechanics states. Performing this first reduction step with the purely structural equations more radically (with low-frequency limit or using balanced reduction) can lead into errors due to subsequent modal aerodynamic coupling effects. Modes that are unimportant for inputs and outputs, that is, with low controllability and observability measures, may be important later for the aeroelasticity.

The model after the first reduction step is used for the derivation of generalized aerodynamic forces, including gust forces. Consequently, the complex model includes all flight mechanics states, all lag states, and the states of the preserved elastic modes. This complex model is further reduced based on the balanced reduction or using other methods as described within the further paragraphs. The final process of reduction is significantly influenced by the necessity of generation of the widely parameterized model, where the unambiguous continuation and tracking of particular states in the process of parameters variation is problematic. This inconvenience is especially substantial for the states corresponding to the elastic modes.

In any case, the result is the set of reduced models for the discrete values of parameters $\mathbf{p}_\mathrm{d}$ in the state-space form.

$$\begin{aligned} \dot{\mathbf{x}}_\mathrm{F} &= \mathbf{A}(\mathbf{p}_\mathrm{d})\mathbf{x} + \mathbf{B}(\mathbf{p}_\mathrm{d})\mathbf{u} \\ \mathbf{y} &= \mathbf{C}(\mathbf{p}_\mathrm{d})\mathbf{x} + \mathbf{D}(\mathbf{p}_\mathrm{d})\mathbf{u} \end{aligned} \tag{4.2}$$

Finally, a set of reduced models is replaced by one model with system parameters that are continuous functions of the parameter vector $\mathbf{p}$. The system parameters will be functions of parameters $\mathbf{p}$ in a form of rational functions.

$$\begin{aligned} \dot{\mathbf{x}}_\mathrm{F} &= \mathbf{A}(\mathbf{p})\mathbf{x} + \mathbf{B}(\mathbf{p})\mathbf{u} \\ \mathbf{y} &= \mathbf{C}(\mathbf{p})\mathbf{x} + \mathbf{D}(\mathbf{p})\mathbf{u} \end{aligned} \tag{4.3}$$

Such parameterized ROM can be processed by the Linear Fractional Transformation (LFT).

4.1.2 First Level of Model Reduction—Modal Reduction of Full Structural Model

4.1.2.1 Modal Decomposition

The basic operation of this decomposition is the well-known modal transformation and sequencing of the eigenfrequencies and corresponding modal coordinates. Starting from

$$\mathbf{M}\ddot{\mathbf{x}} + \mathbf{B}\dot{\mathbf{x}} + \mathbf{K}\mathbf{x} = \mathbf{f}, \tag{4.4}$$

the corresponding modal transformation $\mathbf{x} = \mathbf{V}\mathbf{q}$ and left multiplication by the modal matrix $\mathbf{V}^{\mathrm{T}}$ of (4.4) leads to

$$\mathbf{V}^{\mathrm{T}}\mathbf{M}\mathbf{V}\ddot{\mathbf{q}} + \mathbf{V}^{\mathrm{T}}\mathbf{B}\mathbf{V}\dot{\mathbf{q}} + \mathbf{V}^{\mathrm{T}}\mathbf{K}\mathbf{V}\mathbf{q} = \mathbf{V}^{\mathrm{T}}\mathbf{f}. \tag{4.5}$$

The elastic part (which belongs to nonzero eigenfrequencies) of the modal matrix $\mathbf{V}_{\mathrm{elast}}$ has been evaluated concerning the mass matrix normalization

$$\mathbf{V}_{\mathrm{elast}}^{\mathrm{T}}\mathbf{M}\mathbf{V}_{\mathrm{elast}} = \mathrm{I}. \tag{4.6}$$

The diagonal matrix of the structures eigenfrequencies $\boldsymbol{\Omega}$ in rad/s is then computed as

$$\mathbf{V}_{\mathrm{elast}}^{\mathrm{T}}\mathbf{K}\mathbf{V}_{\mathrm{elast}} = \boldsymbol{\Omega}^2. \tag{4.7}$$

Concerning proportional damping, also the third part of the equation system is diagonalized

$$\mathbf{V}_{\mathrm{elast}}^{\mathrm{T}}\mathbf{B}\mathbf{V}_{\mathrm{elast}} = 2\mathbf{b}_{\mathrm{d}}\boldsymbol{\Omega}, \tag{4.8}$$

where $\mathbf{b}_{\mathrm{d}}$ is the diagonal matrix of the modal damping ratios of separate eigenfrequencies. Concerning the flexible modes reduction, the first step of reduction simply preserves the eigenmodes corresponding to lowest eigenfrequencies bellow some chosen limit.

4.1.2.2 Computation of Rigid Body Modes

As mentioned above, all RB modes of the structure have to be included, since they are base for the flight mechanics states. The simplest version of the RB modes includes vertical (z-direction) and lateral (y- and x-direction) translations as well as roll, yaw and pitch rotation. Additional RB modes of the model are the deflections of control surfaces. Global RBM (structure as a whole), included in the modal basis, neither

have structural stiffness nor structural damping. The local RB modes (flaps, ailerons) may receive structural stiffness and damping if required. The RB modes describe the motion of the whole body without deformation. The correct RB modes applied to system coordinates must not induce elastic forces. This crucial property can simply be written in matrix form

$$\mathbf{K}\mathbf{V}_{\text{rigid}} = \mathbf{0}. \tag{4.9}$$

The RB modes are actually a special case of static constraint modes rather than the eigenmodes [2]. Based on this consideration, the RB modes can be evaluated based on

$$\begin{bmatrix} \mathbf{K}_{ii} & \mathbf{K}_{ir} \\ \mathbf{K}_{ri} & \mathbf{K}_{rr} \end{bmatrix} \begin{bmatrix} \mathbf{V}_{ir} \\ \mathbf{V}_{rr} \end{bmatrix} = \begin{bmatrix} \mathbf{0}_{ir} \\ \mathbf{0}_{rr} \end{bmatrix}. \tag{4.10}$$

The index r denotes an arbitrary set of coordinates $\mathbf{z}_{\text{rigid}}$ that is just sufficient to restrain RB motion of the system. The RB modes can be computed equating $\mathbf{V}_{rr} = \mathrm{I}_{rr}$ (each mode corresponds to particular coordinate from the set $\mathbf{z}_{\text{rigid}}$). The rest of RB mode elements can be evaluated afterwards from (4.10) as

$$\mathbf{V}_{ir} = \mathbf{K}_{ii}^{-1}\left(-\mathbf{K}_{ir}\mathbf{V}_{rr}\right) = \mathbf{K}_{ii}^{-1}\left(-\mathbf{K}_{ir}\right) \tag{4.11}$$

The complete motion in physical coordinates can be evaluated using the superposition of RB motion and flexible modes vibrations

$$\mathbf{x} = \mathbf{x}_r + \mathbf{x}_e = \mathbf{V}_{\text{rigid}}\mathbf{z}_{\text{rigid}} + \mathbf{V}_{\text{elast}}\mathbf{q}_{\text{elast}}. \tag{4.12}$$

Concerning condition of RB motion (4.9) the dynamic equations for the RB coordinates accelerations are

$$\mathbf{V}_{\text{rigid}}^{\text{T}}\mathbf{M}\mathbf{V}_{\text{rigid}}\ddot{\mathbf{z}}_{\text{rigid}} = \mathbf{V}_{\text{rigid}}^{\text{T}}\mathbf{f} \tag{4.13}$$

$$\ddot{\mathbf{z}}_{\text{rigid}} = \mu_{\text{rigid}}^{-1}\mathbf{V}_{\text{rigid}}^{\text{T}}\mathbf{f}, \quad \mu_{\text{rigid}} = \mathbf{V}_{\text{rigid}}^{\text{T}}\mathbf{M}\mathbf{V}_{\text{rigid}}. \tag{4.14}$$

4.1.2.3 Computation of Residual Modes

The cutoff eigenmodes which are not included in the ROM can be represented by the residual mode, which represents the feedthrough components. Strictly speaking, it is the application of the general SPA for the system described by the modal coordinates. The including of the residual mode is important for better preservation of the frequency value of the original system zeros (antiresonances). The reliability of the antiresonances is important for the feedback loop properties [18]. The structural part of the aircraft model is a free body including 6 RB modes, accordingly the flexibility

matrix $\mathbf{G} = \mathbf{K}^{-1}$ does not exist and the residual mode must be computed using the inertia-relief projection matrix [2, 18]. Concerning decomposition (4.12) and RB motion condition (4.9) the complete dynamic equation is

$$\mathbf{M}\mathbf{V}_{\text{rigid}}\ddot{\mathbf{z}}_{\text{rigid}} + \mathbf{M}\mathbf{V}_{\text{elast}}\ddot{\mathbf{q}}_{\text{elast}} + \mathbf{B}\mathbf{V}_{\text{elast}}\dot{\mathbf{q}}_{\text{elast}} + \mathbf{K}\mathbf{V}_{\text{elast}}\mathbf{q}_{\text{elast}} = \mathbf{f} \tag{4.15}$$

substitution from (4.14) the equation can be rewritten into the form

$$\begin{aligned}\mathbf{M}\mathbf{V}_{\text{elast}}\ddot{\mathbf{q}}_{\text{elast}} + \mathbf{B}\mathbf{V}_{\text{elast}}\dot{\mathbf{q}}_{\text{elast}} + \mathbf{K}\mathbf{V}_{\text{elast}}\mathbf{q}_{\text{elast}} &= \mathbf{f} - \mathbf{M}\mathbf{V}_{\text{rigid}}\mu_{\text{rigid}}^{-1}\mathbf{V}_{\text{rigid}}^{\text{T}}\mathbf{f} \\ &= \left(\mathrm{I} - \mathbf{M}\mathbf{V}_{\text{rigid}}\mu_{\text{rigid}}^{-1}\mathbf{V}_{\text{rigid}}^{\text{T}}\right)\mathbf{f}\end{aligned} \tag{4.16}$$

The matrix $\mathbf{P}^{\text{T}} = \mathrm{I} - \mathbf{M}\mathbf{V}_{\text{rigid}}\mu_{\text{rigid}}^{-1}\mathbf{V}_{\text{rigid}}^{\text{T}}$ is the so-called inertia-relief projection matrix. The matrix $\mathbf{P}$ operates as a filter which leaves unchanged the flexible modes and destroys RB modes. $\left(\mathrm{I} - \mathbf{M}\mathbf{V}_{\text{rigid}}\mu_{\text{rigid}}^{-1}\mathbf{V}_{\text{rigid}}^{\text{T}}\right)\mathbf{f} = \mathbf{P}^{\text{T}}\mathbf{f}$ is self-equilibrated superposition of the external forces and inertia forces from RB motion of the body. Thanks to the self-equilibrium and filter properties of $\mathbf{P}$, the self-equilibrium position in elastic physical coordinates can be written as

$$\mathbf{x}_e = \mathbf{P}\mathbf{G}_{ii}\mathbf{P}^{\text{T}}\mathbf{f} \tag{4.17}$$

$\mathbf{G}_{ii}$ is the flexibility matrix corresponding to arbitrary virtual suspension which restrain the RB motion. In our Nacre model, we have used again the suspension described in previous paragraph, $\mathbf{G}_{ii} = \mathbf{K}_{ii}^{-1}$.

The resulting residual matrix can be evaluated as

$$\mathbf{R} = \sum_{k=m+1}^{\infty} \frac{\mathbf{V}_{\text{elast},k}\mathbf{V}_{\text{elast},k}^{\text{T}}}{\Omega_k^2} = \mathbf{P}\mathbf{G}_{ii}\mathbf{P}^{\text{T}} - \sum_{j=1}^{m} \frac{\mathbf{V}_{\text{elast},j}\mathbf{V}_{\text{elast},j}}{\Omega_j^2} \tag{4.18}$$

where m is the number of nonzero eigenfrequencies retained in the ROM.

4.1.3 Second Level of Model Reduction—Reduction of Complete Aeroelastic Model

As mentioned above, the model after the first level of reduction is used for the preparation of the complete aeroelastic model including all flight mechanics states, all lag states, the states of the preserved elastic modes, and possibly also the residual mode. Preparation of this complex model is described in the Sects. 3.3–3.5. The second level of reduction is realized on this complex model.

There are several methods how to prepare the ROM of the system suitable for the control algorithm design [4, 13, 22]. Despite different reduction concepts being

used, there are always two basic possibilities: the state truncation (ST) or the SPA. Let the original state-space model be divided as follows (states corresponding to index 1 are the preserved ones, 2 are the eliminated ones):

$$\mathrm{SS}_{\mathrm{orig}} = \begin{bmatrix} \mathbf{A}_{11} & \mathbf{A}_{12} & \mathbf{B}_1 \\ \mathbf{A}_{21} & \mathbf{A}_{22} & \mathbf{B}_2 \\ \mathbf{C}_1 & \mathbf{C}_2 & \mathbf{D} \end{bmatrix}. \tag{4.19}$$

Then, the reduced-order state-space model obtained by ST of any type is

$$\mathrm{SS}_{\mathrm{trunc}} = \begin{bmatrix} \mathbf{A}_{11} & \mathbf{B}_1 \\ \mathbf{C}_1 & \mathbf{D} \end{bmatrix}. \tag{4.20}$$

The SPA variant of the reduced model preserves the static gains (DC gain) of an original system and generally can be written as

$$\mathrm{SS}_{\mathrm{spa}} = \begin{bmatrix} \mathbf{A}_{11} - \mathbf{A}_{12}\mathbf{A}_{22}^{-1}\mathbf{A}_{21} & \mathbf{B}_1 - \mathbf{A}_{12}\mathbf{A}_{22}^{-1}\mathbf{B}_2 \\ \mathbf{C}_1 - \mathbf{C}_2\mathbf{A}_{22}^{-1}\mathbf{A}_{21} & \mathbf{D} - \mathbf{C}_2\mathbf{A}_{22}^{-1}\mathbf{B}_2 \end{bmatrix}. \tag{4.21}$$

The preserving of the transfer functions for DC gain and for the low frequencies is important in the context of the low-order model approximation and consequently preserving of the RB and flight dynamics motion components. Therefore, the SPA [21] variant of the reduction has been preferentially chosen.

4.1.4 Balanced Reduction

The important concept of the generation of the ROM is the balanced reduction [13] based on the given inputs and outputs with the chosen model dimension. The balanced reduction has been used as the reference one. The general methods of the balanced reduction are based on solution of Lyapunov equation [4, 13]. The basic algorithm of the balanced ROM generation is as follows [4]. The unstable part of the original system must be included also in the ROM. The reduction is applied only to stable part of the system. Let the original system in the state-space form be

$$\mathrm{SS} = \begin{bmatrix} \mathbf{A} & \mathbf{B} \\ \mathbf{C} & \mathbf{D} \end{bmatrix}. \tag{4.22}$$

$$\mathrm{SS}_{\mathrm{b}} = \begin{bmatrix} \mathbf{Z}^{-1}\mathbf{A}\mathbf{Z} & \mathbf{Z}^{-1}\mathbf{B} \\ \mathbf{C}\mathbf{Z} & \mathbf{D} \end{bmatrix} = \begin{bmatrix} \mathbf{A}_{11} & \mathbf{A}_{12} & \mathbf{B}_1 \\ \mathbf{A}_{21} & \mathbf{A}_{22} & \mathbf{B}_2 \\ \mathbf{C}_1 & \mathbf{C}_2 & \mathbf{D} \end{bmatrix}. \tag{4.23}$$

The similarity transformation matrix $\mathbf{Z}$ is formally decomposed with regard to partitioning of the state matrix

$$\mathbf{Z} = \begin{bmatrix} \mathbf{T}, \mathbf{U} \end{bmatrix}, \quad \mathbf{Z}^{-1} = \begin{bmatrix} \mathbf{L} \\ \mathbf{V} \end{bmatrix} \tag{4.24}$$

The balancing-related model reduction methods are connected with the so-called controllability and observability gramians $\mathbf{P}$ and $\mathbf{Q}$ which can be computed from a pair of Lyapunov equations

$$\begin{aligned} \mathbf{AP} + \mathbf{PA}^{\mathrm{T}} + \mathbf{BB}^{\mathrm{T}} &= \mathbf{0} \\ \mathbf{A}^{\mathrm{T}}\mathbf{Q} + \mathbf{QA} + \mathbf{C}^{\mathrm{T}}\mathbf{C} &= \mathbf{0} \end{aligned} \tag{4.25}$$

The gramians of a stable system are positive semidefinite matrices which can be decomposed by Cholesky factorization $\mathbf{P} = \mathbf{SS}^{\mathrm{T}}$ and $\mathbf{Q} = \mathbf{R}^{\mathrm{T}}\mathbf{R}$. So-called Hankel singular values of the system are obtained by singular value decomposition

$$\mathbf{RS} = \begin{bmatrix} \mathbf{U}_1 \ \mathbf{U}_2 \end{bmatrix} \begin{bmatrix} \Sigma_1 & \mathbf{0} \\ \mathbf{0} & \Sigma_2 \end{bmatrix} \begin{bmatrix} \mathbf{V}_1 \\ \mathbf{V}_2 \end{bmatrix} \tag{4.26}$$

The singular values are ordered, first r largest singular values in $\mathbf{\Sigma}_1$ correspond to retained states, the rest $\mathbf{\Sigma}_2$ correspond to neglected states.

$$\mathbf{L} = \mathbf{\Sigma}_1^{-1/2}\mathbf{U}_1^{\mathrm{T}}\mathbf{R}, \quad \mathbf{T} = \mathbf{SV}_1\mathbf{\Sigma}_1^{-1/2} \tag{4.27}$$

The balanced reduction is very straightforward especially for the pure structural models with the proportional damping. The airplane model, however, also consists of the states with the high damping and even real poles. The evaluation of the final damping values of particular modes is relatively complex. The computational experiments show that the pure balanced reduction can discard some important states, like the first bending mode, some of the lag states, or even some flight mechanics states. Consequently, the combined reduction approaches have been tested.

4.1.4.1 Combined Model Reduction

Based on the control design requirements, the second level model has been reduced in two main versions. The first (control design) ROM contains all flight mechanics states, lag states and states of the first (lowest) 4 elastic modes. The SPA variant of the reduction has been chosen. The set of the small (4 elastic modes) models is prepared in the grid version and also in the parameterized version as described in the next paragraph about parameterization. In concrete, the 5th order of polynomial parameterization has been chosen. Besides the small model with 4 elastic modes,

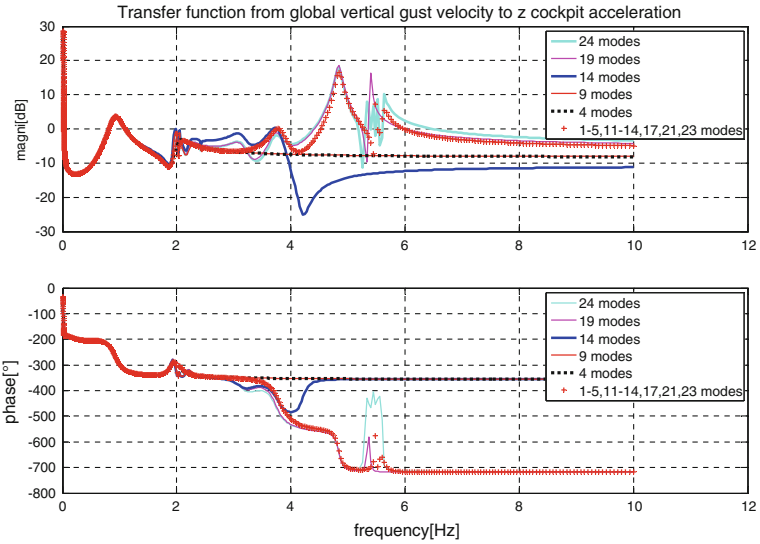

Fig. 4.1 TF from global vertical gust to z cockpit acceleration

also the larger testing model with selected set of 12 elastic modes or 19 elastic modes has been tested.

The choice starts from the balanced reduction and is modified based on the inspection of comparisons of many transfer functions for different levels of reduction (with first 4 elastic modes, first 9 elastic modes, first 14 elastic modes, first 19 elastic modes, first 24 elastic modes). The SPA variant of reduction has been chosen. The examples of the transfer functions are in Figs. 4.1 and 4.2. The larger model has been primarily prepared only in the grid version, the problems of tracking, and the final solution is described in next paragraphs.

4.1.5 Parameterization of Aircraft Models

The result of the reduction process is the set of reduced models (4.3) that are known for the values of parameters $\mathbf{p}_\mathrm{d}$. These models for the discrete values of parameters are to be replaced by one model the system parameters of which are some approximation continuous functions of the parameters. The system parameters are the elements of the system matrices $\mathbf{A}, \mathbf{B}, \mathbf{C}, \mathbf{D}$. The form of the approximation function must be a rational function, that is, a fraction of two polynomial functions. There are two groups of methods for construction of such approximations.

The first group is the approximation by splines and the second group is the approximation by radial basis functions (RBF). It is considered four parameters $\mathbf{p}_\mathrm{d}$

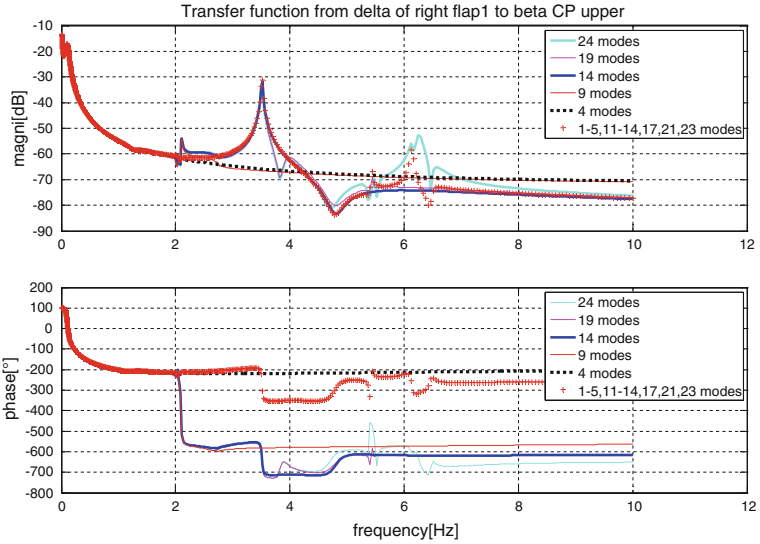

Fig. 4.2 TF from angle of right flap 1 to upper cockpit side-slip angle

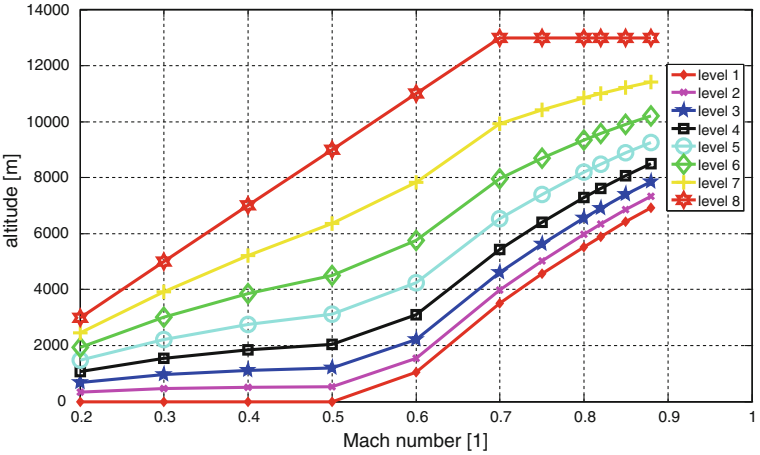

Fig. 4.3 Values of considered altitude levels and Mach numbers

- I_{Pass}—the number of the *passenger* variant (1, 2, 3)
- I_{Fuel}—the number of the *fuel* variant (1, 2, 3, 4, 5, 6, 7)
- I_{Mach}—the number of the *Mach* variant (1, 2, 3, 4, 5, 6, 7, 8, 9, 10, 11)
- I_{Alti}—the number of the *altitude level* variant (1, 2, 3, 4, 5, 6, 7, 8).

Values of considered altitude levels and Mach numbers are presented in Fig. 4.3.

4.1.6 Spline Interpolation

The splines can be divided into polynomial splines and rational splines (fraction of two polynomial splines). Each parameter p_i has the span $p_{i0} < p_i < p_{in_i}$ and the span is divided into n_i intervals $[p_{i,k-1}, p_{i,k}]$ in such way that $p_{i0} < p_{i1} < \cdots < p_{i,k-1} < p_{i,k} < \cdots < p_{i,n_i}$. The Cartesian product of the span consists of the Cartesian product of subintervals and each such Cartesian product of subintervals is for the system parameter S approximated by the Cartesian product of cubic polynomial splines

$$S = \sum_{i1=0}^{3} \sum_{i2=0}^{3} \sum_{i3=0}^{3} \sum_{i4=0}^{3} S_{i1,i2,i3,i4} p_1^{i1} p_2^{i2} p_3^{i3} p_4^{i4} \tag{4.28}$$

or by the Cartesian product of cubic rational splines

$$S = \frac{\sum_{i1=0}^{3} \sum_{i2=0}^{3} \sum_{i3=0}^{3} \sum_{i4=0}^{3} S^N_{i1,i2,i3,i4} p_1^{i1} p_2^{i2} p_3^{i3} p_4^{i4}}{\sum_{i1=0}^{3} \sum_{i2=0}^{3} \sum_{i3=0}^{3} \sum_{i4=0}^{3} S^D_{i1,i2,i3,i4} p_1^{i1} p_2^{i2} p_3^{i3} p_4^{i4}} \tag{4.29}$$

The particular splines can be created using the theory of geometric parametric splines for curves and surfaces like as B-splines and NURBS. The requirements on the approximation properties are here much fewer than in geometry.

4.1.6.1 Radial Basis Functions

The approximation by the RBF is based on the idea that the approximated function is approximated by the sum of its values (or weights) multiplied by the distance function from the function input. In the case of the system parameter S the approximation is

$$S = \sum_K S_K \Phi \left(\| \mathbf{p}_K - \mathbf{c}_K \| \right) \tag{4.30}$$

where Φ is the distance function, $\mathbf{c}_K$ is the input center, S_K the values or weights of the function. The distance functions are usually Gaussian functions. This theory has been developed specifically for system model approximations in the system LOLIMOT [12]. This original system has been reimplemented and extended at CTU [20] and modified by replacement of the Gaussian function by rational functions for the distance

$$\Phi \left(\| \mathbf{p}_K - \mathbf{c}_K \| \right) = \prod_K \frac{1}{\sum_{i=0}^{n} \left(\frac{p_K - c_K}{\sqrt{2}\sigma_K} \right)^{2n} \frac{1}{n!}} \tag{4.31}$$

The developed software CTU-MIMO-POLYNOMIAL-LOLIMOT has been used for continuous multidimensional approximation of the grid point data. CTU-MIMO-POLYNOMIAL-LOLIMOT in basic form generates approximation of any function in parameters p by locally linear functions and globally rational functions. For example, the formula for three dimensional parameterization ($\mathbf{p} = [p_1, p_2, p_3]^{\mathrm{T}}$) has a form

$$\begin{aligned} S &= \sum_{k=1}^{m} (w_{k,0} + w_{k,1} p_1 + w_{k,2} p_2 + w_{k,3} p_3) \Phi\left(\|\mathbf{p} - \mathbf{c}_k\|\right) \\ &= \sum_{k=1}^{m} (w_{k,0} + w_{k,1} p_1 + w_{k,2} p_2 + w_{k,3} p_3) \prod_{j=1}^{3} \frac{1}{\sum_{i=0}^{n} \left(\frac{p_j - c_{k,j}}{\sqrt{2}\sigma_K}\right)^{2i} \frac{1}{i!}} \end{aligned} \tag{4.32}$$

The local linear function can be generalized to local polynomial n-dimensional function

$$\begin{aligned} \mathrm{pol}(p_1, p_2, p_3) = w_{k,0} + w_{k,1} p_1 + w_{k,2} p_2 + w_{k,3} p_3 \\ + w_{k,4} p_1^2 + w_{k,5} p_2^2 + w_{k,6} p_3^2 + w_{k,7} p_1 p_2 + \cdots \end{aligned} \tag{4.33}$$

and if possible from the point of view of accuracy, one polynomial function can be used for the whole parameter interval. So, we can switch between these (rational/polynomial) types of approximation. The inherent trade-off between accuracy and complexity needs to be considered.

4.1.6.2 Parametrization Problems

The parametrization described in previous section can enter three kinds of problems. The first kind of problems is with the continuity of reduced coordinates. The reduction process can result into different coordinates for different values of parameters $\mathbf{p}_\mathrm{d}$. Such situation is presented in Fig. 4.4. The modal coordinates chosen to ROM by balanced reduction are marked by circles. The choices for the variant 00 (no fuel, no passengers) and for the variant 44 (full fuel tanks, all passengers) are different.

This results into discontinuities of the system parameters in model description $\mathbf{A}, \mathbf{B}, \mathbf{C}, \mathbf{D}$. Such parameterized ROM cannot be controlled. The change of coordinates within the reduction process for different values of parameters $\mathbf{p}_\mathrm{d}$ must be avoided. This means that many reduction techniques that are very efficient from the point of view of accurate reduction cannot be used.

The second kind of problems is with the parametrization of ROM between the values of parameters $\mathbf{p}_\mathrm{d}$. The parametrization can be separately very good, but the parameterized ROM between the values of parameters $\mathbf{p}_\mathrm{d}$ can be wrong. For example, the parameterized ROM model can be unstable between the values of parameters $\mathbf{p}_\mathrm{d}$.

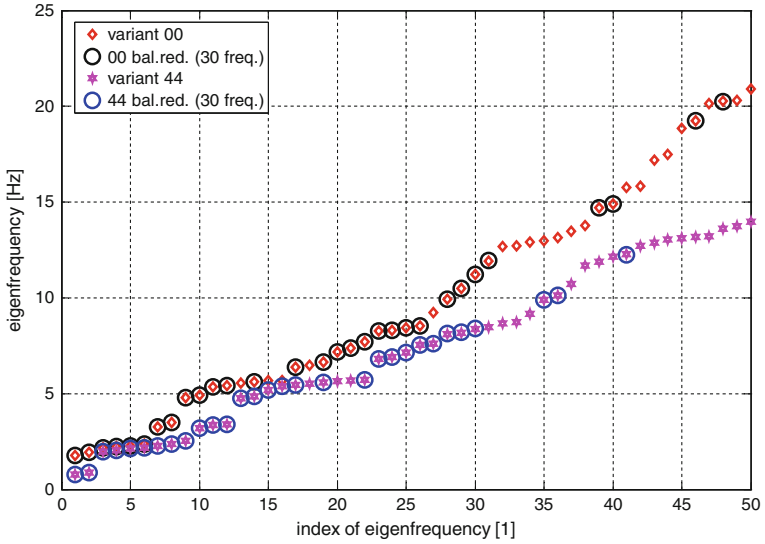

Fig. 4.4 Choice of modes to ROM for different variants based on balanced reduction

It is necessary to test basic properties (eigenvalues, stability, controllability, observability) for the interpolated matrices between original grid points.

The third kind of problems is the unique tracking of corresponding states during the parameters change. This problem is particularly problematic for the states corresponding to elastic modes. The modal assurance criterion can be used for testing of proximity of eigenmodes in adjacent grid points, but the reliable identification and tracking of all states across the wide parameter intervals is not easy. The final solution used within the project test gradually the consistency of states across all variants for the increasing number of preserved states.

4.1.7 Conclusion

The finally chosen solution of the reduction process comes from the testing of many variants and is highly influenced by the request of internally consistent parameterized model. The first level ROMs have been prepared with the 80 states. The second level of reduction process ends with two variants of models. The first variant of the control design ROM contains all flight mechanics states, all lag states, and states of the first (lowest) 19 elastic modes. The simplified variant of the control design ROM takes separately the symmetric and skew-symmetric component including all flight mechanics states, all lag states, and states of the first (lowest) 4 elastic modes. The example of comparison between original (80 states) and reduced input–output (only 2 symmetric modes) transfer function is in Fig. 4.5.

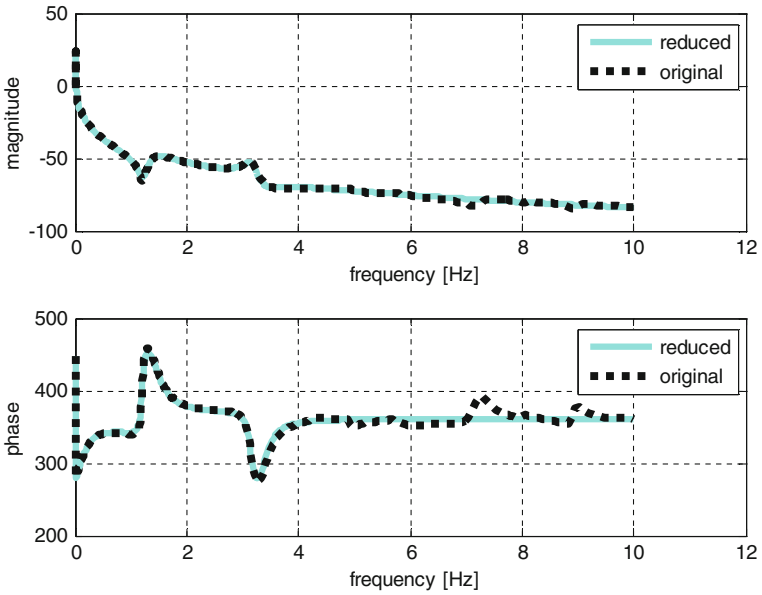

Fig. 4.5 Example of comparison between original and reduced transfer function

4.2 Linear Fractional Representation of Parametrized Models

S. Hecker

Over the last 20 years, a paradigm shift in the modeling of dynamic systems occurred with the introduction of modern robust control theory and its associated modeling framework, the LFT [14, 15]. A Linear Fractional Representation (LFR) is a representation of a nonlinear system as a linear system formed by a constant M matrix in linear feedback with a structured matrix $\mathbf{\Delta}$. The process of extracting the uncertainty into the structured matrix $\mathbf{\Delta}$ of this so-called $M - \mathbf{\Delta}$ form is called LFR realization, also known as "pulling out the delta", and is considered the fundamental LFR modeling step. From these initial LFT developments, it was immediately recognized that they were part of the larger set of linear parameter-varying (LPV) models but presenting a specific structure. This generated great interest and sparked the development of the (LPV)/(LFT) field [10, 11, 14–16, 19, 24].

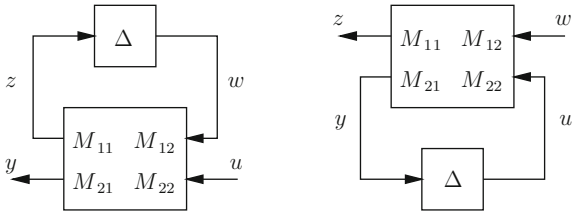

Fig. 4.6 Graphical representation of lower and upper LFTs

4.2.1 Linear Fractional Transformation

A LFT is a matrix function based on two matrix components,

$$\mathbf{M} = \begin{bmatrix} \mathbf{M}_{11} & \mathbf{M}_{12} \\ \mathbf{M}_{21} & \mathbf{M}_{22} \end{bmatrix}$$

and $\mathbf{\Delta}$, and a feedback interconnection. The matrix $\mathbf{M}$ represents the nominal, known, part of the system, while the matrix $\mathbf{\Delta}$ contains the time-varying, unknown, or uncertain components.

Depending on the feedback interconnection used, there are two possible types of LFTs, upper [see Fig. 4.6-left and (4.34)] and upper [see Fig. 4.6-right and (4.35)].

$$\mathscr{F}_{\mathrm{u}}(\mathbf{M}, \mathbf{\Delta}) = \mathbf{M}_{22} + \mathbf{M}_{21}(\mathrm{I} - \mathbf{\Delta}\mathbf{M}_{11})^{-1}\mathbf{\Delta}\mathbf{M}_{12} \tag{4.34}$$

$$\mathscr{F}_{\mathrm{l}}(\mathbf{M}, \mathbf{\Delta}) = \mathbf{M}_{11} + \mathbf{M}_{12}(\mathrm{I} - \mathbf{\Delta}\mathbf{M}_{22})^{-1}\mathbf{\Delta}\mathbf{M}_{21} \tag{4.35}$$

Remark 1 The matrix $\mathbf{\Delta}$ is typically norm-bounded $\|\mathbf{\Delta}\|_\infty \leq 1$ for design and analysis (without loss of generality by scaling of $\mathbf{M}$), but otherwise unrestricted in form (structured/unstructured) or type (nonlinear/time-varying/constant). If any of the components in $\mathbf{\Delta}$ is a scheduling parameter, an LPV system is obtained.

Remark 2 The order of the LFR is the number of parameters, including repetitions, contained in $\mathbf{\Delta}$ (for example, $\mathbf{\Delta} = \mathrm{diag}(p_1\mathrm{I}_2, p_2) \rightarrow$ LFR order is 3). Since many realistic robustness analysis problems can easily result in very-high-order LFRs, it is vital to have efficient and automated tools which can compute minimal, or at least close to minimal, representations of these systems.

Remark 3 A very important property of LFRs is that their interconnection results in another LFR (for example, sum, concatenation, etc. of LFRs result in LFRs) [5, 10].

4.2.2 Process of LFR Modeling

The most widespread, standard approach to obtain an LFR is based on the numerical Jacobian LPV approach augmented with the final LFR realization step of "pulling out the deltas". Hence the basis for the LFR modeling is a set of linear time-invariant (LTI) models generated by trimming and linearizing a nonlinear aircraft model at specific points within the flight envelope (Mach number and dynamic pressure) and for different parameter values (in ACFA2020 the fuel mass and center of gravity (CG) position parameters). These grid-point models are then interpolated using polynomial functions to obtain one single LPV model describing the full set of LTI models. Finally, the LPV model is transformed into an LFR.

This approach has the advantages of relying on well-known numerical techniques (to obtain equilibrium points and linearizations of plants) and of resulting in purely LTI models (once the components in the $\mathbf{\Delta}$ matrix are assigned numerical values). These advantages are highly relevant since most engineers are acquainted with numerical linearization and with linear analysis/synthesis techniques which are applicable due to the underlying LTI nature of the LFR. The drawback is a loss of modeling oversight as application of the numerical trim/linearization step transforms the modeling problem into a numerical black box approach. Furthermore, the results obtained from LTI synthesis/analysis need to be validated on the purely nonlinear model and there may exist a wide gap between the latter and the linear models used for design. The LFR modeling can be summarized in the following five-step process:

1. *Trimming and linearization*: the nonlinear aircraft model is trimmed and linearized at several values of the parameter vector $p = (p_1, \ldots, p_4)$, were the uncertain parameters are the fuel case (p_1 with 11 grid points), the position of center of gravity (p_2 with 3 grid points), the Mach number (p_3 with 8 grid points) and the dynamic pressure (p_4 with 13 grid points). The result was a set of 3432 LTI models.
2. *Model interpolation*: in order to accurately approximate the grid point LTI models with an LPV model, a usual way is to generate multivariable polynomials for all varying entries of the LTI state-space matrices $\mathbf{A}, \mathbf{B}, \mathbf{C}, \mathbf{D}$. This may result in very complex polynomial LPV models, which then may yield high-order LFRs. To avoid this, a general approach is presented in [17] to generate an LPV model, which approximates a set of linearized grid-point models with high accuracy and is optimally suited for LFT-based Robust Stability (RS) analysis and control design. The idea is to combine the polynomial fitting with a global optimization where the objective is to find an LPV model, which has the property to allow a transformation into an LFR of lowest possible order. A gap metric constraint is included during the optimization in order to guarantee a specified accuracy of the transfer function of the LPV model. As a result, only the varying state-space matrix entries that have a significant influence on the transfer function are fitted with polynomials, whereas the others are taken constant. In addition, the number of required monomials within each polynomial is optimized in order to

reduce complexity. Some recent applications [9, 17] of the method have shown its effectiveness.

3. *Symbolic preprocessing*: the role of symbolic preprocessing is to find equivalent representations of individual matrix elements, entire rows/columns or even the whole parametric state-space matrices, which lead to LFRs of lower order when realized with the object-oriented LFT realization approach. There exist many methods [8] such as the Horner form transformation, the structured tree decomposition [1], and the variable splitting factorization [7].
4. *Object-oriented LFR realization*: the method is described in [10] and in [5] it is extended to allow direct LFR realization of general rational parametric systems. The basic idea is to realize elementary LFRs for each uncertain parameter and to use basic LFR manipulation formulas for addition, subtraction, multiplication, inversion and row/column concatenation to build an LFR for a rational parametric matrix. The method is very flexible and can be easily automated, thus allowing an efficient and reliable implementation, which is available within the LFR Toolbox for MATLAB® Version 2 [6].
5. *Numerical order reduction*: in a last step it can be attempted to reduce the order of the LFR by using numerical multidimensional order reduction algorithms [3, 10], which are also implemented in [6]. There are papers [3] that discuss LFR minimality, but that is under the assumption that the uncertain parameters do not commute. The idea behind the numerical 1-D reduction method is to repeatedly perform standard 1-dimensional order reduction for each uncertain parameter. The *n*-D technique [3] works in a similar way but considers all parameters at once, and generally yields LFRs of lower orders compared to the 1D technique.

4.2.3 Generation of LFRs for the ACFA 2020 BWB Aircraft

In this section, the order and structure of the resulting LFRs that were used for controller synthesis are described. As the methods for LFT-based robust controller synthesis are computationally demanding, it is of prior interest to use LFRs of low order. This usually requires to reduce the order and complexity (number of states, inputs and outputs, number of uncertain parameters, number of LTI grid-point models covering a certain region of the flight envelope, …) of the underlying LTI grid-point models that are used for LFR generation.

Here, the ROMs created as outlined in Sect. 4.1 are the starting point to generate LFRs for control design. In the following, longitudinal LFR models are generated for the open-loop aircraft with and without modeled phugoid mode and utilized in system analysis and in the LPV feedback design in Sect. 6.5. Lateral LFR models of the open-loop dynamics controlled by a 1st-order initial stabilizing controller (designed in Sect. 6.2) are generated and utilized in the robust feedback design in Sect. 6.3.

4.2.3.1 A Priori Model Simplifications

The first step in LFR modeling is the interpolation of a set of LTI state-space models using polynomial functions for each element of the state-space system matrices **A**, **B**, **C**, and **D**. Hence the number of states, inputs and outputs, which define the dimension of these matrices play an important role in terms of the resulting LFR order. A lower number of states, inputs and outputs usually results in a lower LFR order. Therefore, in a first step, the overall aircraft model was split into two models describing the longitudinal and lateral dynamics only. In addition, the longitudinal model included only symmetric elastic modes and the lateral model included only asymmetric and antisymmetric elastic modes.

The number of elastic modes that were considered for controller synthesis was also drastically reduced and the LFRs usually included only between 2 and 6 elastic modes of lowest frequencies. Elastic modes of higher frequencies were only used for controller validation but due to the low bandwidth of the actuators and a roll-off of the controller, the excitation of these modes from the controller was very small.

An accurate description of the gust affecting the aircraft dynamics resulted in a large number of lag states that were included in the LTI aircraft models. For controlling the elastic modes, the robust controllers mainly used acceleration sensors, and no feed-forward system using a forward-looking sensor (for example, LIDAR) was used. Therefore, the way (gust or maneuver) and accuracy of how the elastic modes were excited was not of highest importance and most of the lag states could be neglected. The controller synthesis models included two lag states.

Furthermore, the control allocation for the large number of model inputs was usually fixed, that is, all controllers typically deflected several control surfaces in the same way. Hence, these control surfaces can be combined and considered as a single model input, which reduces the number of model inputs (columns in **B** and **D** state-space matrices).

Finally, only six model outputs were chosen for the controller synthesis model from the large number of outputs available from modeling.

The aircraft model includes four uncertain parameters, namely Mach number, position of center of gravity, fuel case, and dynamic pressure. For the LFRs, the Mach number and dynamic pressure were considered fixed and only the fuel case and the position of center of gravity were considered uncertain, resulting in an LFR with only two parameters. A reason for this simplification was that the Mach number and dynamic pressure can me measured very accurately and to high safety levels. Therefore, these parameters are used for gain scheduling, that is, several robust controllers (robust with respect to fuel case and CG position) for different Mach numbers and dynamic pressures will be synthesized and scheduled a posteriori.

4.2.3.2 LFRs for the Longitudinal Aircraft Model

The longitudinal aircraft model includes either 12- or 14- states: four states from two actuator models, two lag states, four states describing the two first (lowest frequency)

symmetric elastic modes and two RB states for the short-period mode. The 14-state model includes two more RB states describing the phugoid mode.

The model has three inputs, where the symmetric deflection of flaps 1 and flaps 2 are combined as one input and the other inputs are the symmetric deflection of flaps 3 and the global vertical gust input.

As outputs we have chosen the vertical load factor Nz_{CG} at the center of gravity, the pitch rate q_{CG} at the center of gravity, the true airspeed V_{TAS}, the combined output $Nz_{\mathrm{long.law}}$, the wing root bending moment M_x (here called M_y) and the vertical cut force Fz at the wing root.

For this model a given cruise condition with fixed Mach number, dynamic pressure and position of center of gravity was chosen and the fuel case parameter is allowed to vary within the full range. Therefore, the resulting LFRs include only one uncertain parameter.

Using the automated generation process described in Sect. 4.2.2, two LFRs were generated for the 14- states model. One accurate model with order 17, that is, $\Delta = p_4\, I_{17}$, and one less accurate model with order 4. During the LFR generation process, the accuracy of the LFR is measured using the ν-gap metric and is given by the maximum ν-gap metric between all the LTI grid-point models (given in the relevant flight domain) and the resulting LFR evaluated at the given grid points. Using the MATLAB® command `gapmetric.m` one obtains a value between 0 and 1, where 0 means that the models are equal and 1 indicates a large difference between the models. For the given LFRs, we obtained values of 0.08 for the accurate model and 0.15 for the less accurate model.

For the 12-state model, an accurate model of order 16 and a less accurate model of order 3 was generated. The maximum errors in terms of the ν-gap metric were given by 0.06 and 0.18.

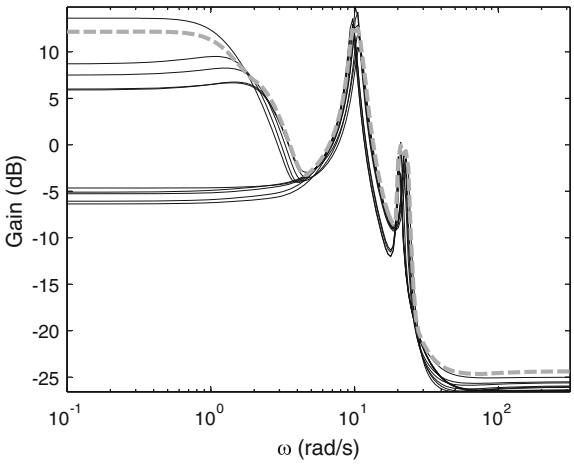

Fig. 4.7 Worst-case gain validation of 12-state model (LFR order 16, no phugoid)

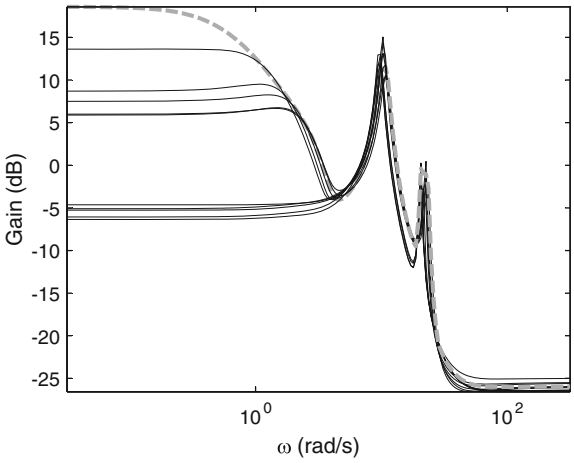

Fig. 4.8 Worst-case gain validation of 12-state model (LFR order 3, no phugoid)

Besides the ν-gap metrics, a further validation of the LFRs was performed by calculating the worst-case gains (MATLAB® function `wcgain.m`) of the LFRs for a given frequency range and comparing these values with the gains (maximum singular value over frequency) of the LTI models. Figures 4.7 and 4.8 show the worst-case gains (dashed gray line) and the gains of the LTI models for the 12-state models. It can be clearly seen that the higher order LFR yield a better approximation/coverage, especially at low and high frequencies the worst-case gain tightly covers the LTI model gains. The low-order LFR overestimates the low-frequency gain and underestimates the gains at the frequency of the first flexible mode. For the 14- states models shown in Figs. 4.9 and 4.10 a better approximation of the higher order LFR can be seen for the low-frequency RB aircraft modes.

4.2.3.3 LFRs for the Lateral Aircraft Model

The lateral aircraft model includes 33- states: six states from three actuator models, no lag states, 18 sensor states, four states describing the two first (lowest frequency) antisymmetric elastic modes, four states for the RB modes and one state for a simple controller that was already included in the model to stabilize the lateral RB modes (designed in Sect. 6.2).

The model has three inputs, where the symmetric deflection of flaps 3 and flaps 4 are combined as one input, the second and third inputs are the rudder and flaps 5.

As outputs, we have chosen the sideslip angle β, the angle φ, the roll rate p, the yaw rate r, the combined output $n_{z_{\text{law,lat}}}$ and the wing root bending moment Mx (here called My).

Two different cruise conditions with fixed Mach number and dynamic pressure were chosen. For the first cruise case, one LFR was generated for the full variation

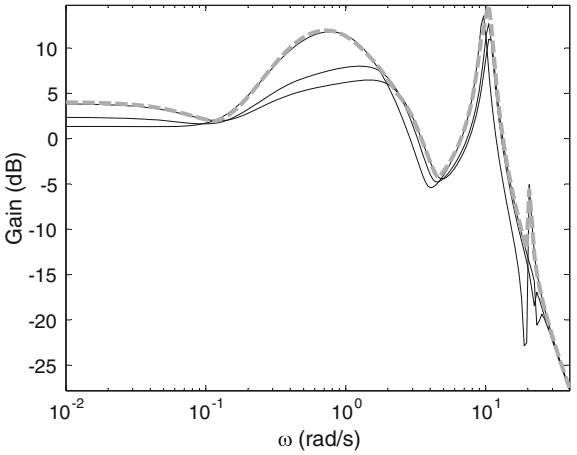

Fig. 4.9 Worst-case gain validation of 14-state model (LFR order 17, with phugoid)

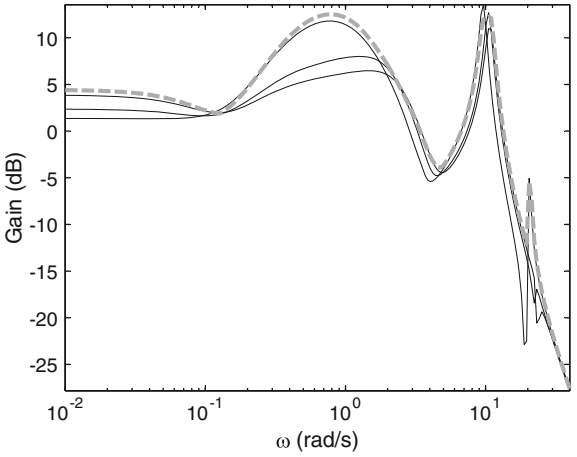

Fig. 4.10 Worst-case gain validation of 14-state model (LFR order 4, with phugoid)

of fuel cases and positions of center of gravity and a second LFR was generated covering all fuel cases but with fixed center of gravity position. For the model with two uncertain parameters, an LFR of order 16 was obtained and for the simpler one-parametric LFR, the order was 4. The corresponding ν-gap metric errors were 0.19 and 0.10. For the second cruise case only a two parametric LFR of order 13 covering all fuel cases and center of gravity positions was generated. The maximum ν-gap metric error of this model was 0.08. Figures 4.11, 4.12 and 4.13 again show that the LFRs tightly cover the LTI models in terms of the worst-case gain. All models were of reasonable complexity to be used for robust control design methods like μ-synthesis (in Sect. 6.3).

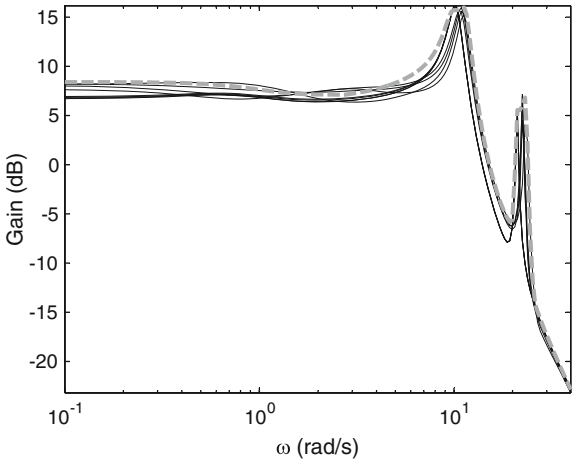

Fig. 4.11 Worst-case gain validation of lateral 33-state model (LFR order 16, parametrized in fuel and CG, cruise case A)

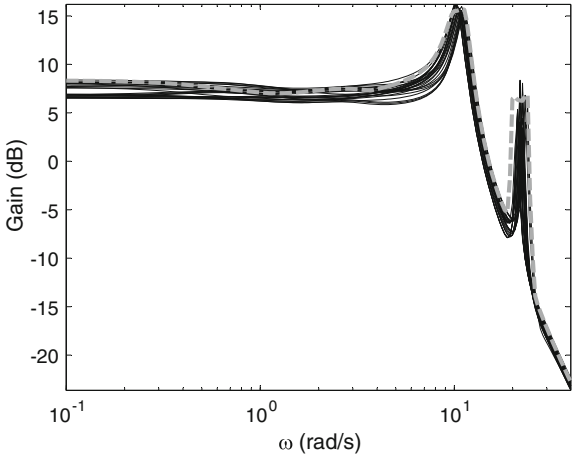

Fig. 4.12 Worst-case gain validation of lateral 33-state model (LFR order 4, parametrized in fuel only, cruise case A)

4.2.4 Summary

For the ACFA 2020 blended wing body (BWB) aircraft, parametric LFRs were generated to be used for robust controller synthesis. During the modeling phase of the project, much effort has been invested in finding models of reasonable complexity which can be used in conjunction with modern robust control design techniques.

One important step toward control-oriented aircraft models was the application of model reduction techniques to reduce the huge number of structural modes in the

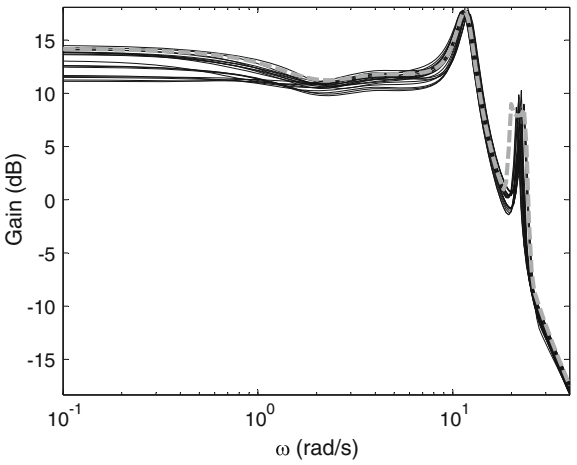

Fig. 4.13 Worst-case gain validation of lateral 33-state model (LFR order 13, parametrized in fuel and CG, cruise case B)

thousands of grid-point LTI models representing the aircraft dynamics for all fuel cases, CG positions, Mach numbers and dynamic pressures. As for LFR generation, the reduced-order grid-point LTI models are interpolated, one has to be very careful to guarantee consistency (number and physical meaning) of the states of the ROMs. Here, it may easily happen that the signs of the elements of the **A**, **B**, and **C** state-space matrices switch from grid point to grid point which does not affect the transfer function of a single grid-point model but makes an interpolation of neighboring grid-point models impossible. During the ACFA project, a fully automated process delivering ROMs that can be interpolated was not available and many sign correction had to be done manually. This is still an open problem and actual research tries to find order-reduction methods that allow the a posteriori interpolation of a set of reduced-order grid-point models [23].

As an alternative to the parametric uncertain models, one may also generate LFRs including an unstructured uncertainty. In this case, the sign problem is not important, however, a lot of structural information is lost and one may obtain more conservative controllers with less performance.

References

1. Cockburn JC, Morton BG (1992) Linear fractional representations of uncertain systems. Automatica 33(7):1263–1271
2. Craig RR (2000) Coupling of substructures for dynamic analyses: an overview. AIAA Paper 1573:2000
3. D'Andrea R, Khatri S (1997) Kalman decomposition of linear fractional transformation representations and minimality. In: Proceedings of the American control conference, Albuquerque, New Mexico, pp 3557–3561

4. Gawronski WK (2004) Advanced structural dynamics and active control of structures. Springer, New York
5. Hecker S, Varga A (2004) Generalized LFT-based representation of parametric uncertain models. Eur J Control 10(4):326–337
6. Hecker S, Varga A, Magni JF (2005) Enhanced LFR-toolbox for MATLAB. Aerosp Sci Technol 9:173–180
7. Hecker S, Varga A (2006) Symbolic techniques for low order LFT-modeling. Int J Control 79(11):1485–1494
8. Hecker S (2007) Generation of low order LFT representations for robust control applications, vol 1114. VDI-Verlag, Düsseldorf
9. Hecker S, Pfifer H (2010) Generation of LFRs for the COFCLUO nonlinear aircraft model. In: 2nd workshop on clearance of flight control laws, Stockholm, Sweden
10. Lambrechts P, Terlouw J, Bennani S, Steinbuch M (1993) Parametric uncertainty modeling using LFTs. In: American control conference, San Francisco
11. Leith DJ, Leithead WE (2000) Survey of gain-scheduling analysis and design. Int J Control 73(11):1001–1025
12. Nelles O (1998) Nonlinear system identification with local linear Neuro-Fuzzy models. PhD thesis, Technische Universitat Darmstadt, Darmstadt
13. Obinata GO, Anderson BDO (2001) Model reduction for control system design, communications and control engineering. Springer, London
14. Packard A, Doyle J (1993) The complex structured singular value. Automatica 29(1):71–109
15. Packard A (1994) Gain scheduling via linear fractional transformations. Syst Control Lett 22:79–92
16. Packard A, Becker G (1994) Robust performance of linear parameter varying systems using parametrically-dependent linear feedback. Syst Control Lett 23:205–215
17. Pfifer H, Hecker S (2008) Generation of optimal linear parametric models for LFT-based robust stability analysis and control design. In: IEEE conference on decision and control (CDC), Cancun, Mexico
18. Preumont A (2002) Vibration control of active structures: an introduction, 2nd edn., Solid mechanics and its application, vol 96. Kluwer Academic Publishers, Dordrecht
19. Shamma J, Cloutier J (1993) Gain-scheduled missile autopilot design using linear parameter varying transformations. J Guid Control Dyn 16(2):256–261
20. Stefan M, Valášek M (2007) CTU-MIMO-POLYNOMIAL-LOLIMOT. FME CTU in Prague, Prague
21. Šika Z, Zavřel J, Valášek M (2009) Residual modes for structure reduction and efficient coupling of substructures. Bull Appl Mech 5(19):54–59
22. Varga A, Anderson BDO (2003) Accuracy-enhancing methods for balancing-related frequency-weighted model and controller reduction. Automatica 39:919–927
23. Vuillemin P, Poussot-Vassal C, Alazard D (2013) A frequency-limited $\mathscr{H}_2$ model approximation method with application to a medium scale flexible aircraft. Euro-GNC, Delft (NL)
24. Wu F, Yang XH, Packard A, Becker G (1996) Induced $\mathscr{L}_2$-norm control for LPV systems with bounded parameter variation rates. Int J Robust Nonlinear Control 6:983–998